



Flavonoid Accumulation Varies in *Medicago truncatula* in Response to Mercury Stress

Gerardo Alvarez-Rivera^{1*†}, Aurora Sanz^{2†}, Alejandro Cifuentes¹, Elena Ibáñez¹, Timothy Paape³, M. Mercedes Lucas² and José J. Pueyo^{2*}

¹ Laboratory of Foodomics, CIAL-CSIC, Institute of Food Science Research, Madrid, Spain, ² Institute of Agricultural Sciences, ICA-CSIC, Madrid, Spain, ³ Brookhaven National Laboratory, Upton, NY, United States

OPEN ACCESS

Edited by:

Sangeeta Dhaubhadel,
Agriculture and Agri-Food Canada,
Canada

Reviewed by:

Junzeng Zhang,
National Research Council Canada
(NRC-CNRC), Canada
Arindam Ghatak,
University of Vienna, Austria
Jian Zhao,
Anhui Agricultural University, China

*Correspondence:

Gerardo Alvarez-Rivera
gerardo.alvarez@csic.es
José J. Pueyo
jj.pueyo@csic.es

[†] These authors share first authorship

Specialty section:

This article was submitted to
Plant Metabolism
and Chemodiversity,
a section of the journal
Frontiers in Plant Science

Received: 30 April 2022

Accepted: 21 June 2022

Published: 07 July 2022

Citation:

Alvarez-Rivera G, Sanz A,
Cifuentes A, Ibáñez E, Paape T,
Lucas MM and Pueyo JJ (2022)
Flavonoid Accumulation Varies
in *Medicago truncatula* in Response
to Mercury Stress.
Front. Plant Sci. 13:933209.
doi: 10.3389/fpls.2022.933209

Mercury (Hg) contamination is increasing worldwide in both wild ecosystems and agricultural soils due to natural processes, but mostly to anthropic activities. The molecular mechanisms involved in Hg toxicity and tolerance in plants have been extensively studied; however, the role of flavonoids in response to Hg stress remains to be investigated. We conducted a metabolomic study to analyze the changes induced at the secondary metabolite level in three Hg-tolerant and one Hg-sensitive *Medicago truncatula* cultivars. A total of 46 flavonoid compounds, classified into five different flavonoid families: anthocyanidins, flavones, isoflavones, pterocarpan flavonoids, and flavanones, along with their respective glycoconjugate derivatives, were identified in leaf and root tissues. The synthesis of free isoflavones, followed by monoglycosylation and further malonylation was shown to be characteristic of root samples, whereas higher glycosylation, followed by further acylation with coumaric and ferulic acid was characteristic of leaf tissues. While minor changes were observed in leaves, significant quantitative changes could be observed in roots upon Hg treatment. Some flavonoids were strongly upregulated in roots, including malonylglucosides of biochanin A, formononetin and medicarpin, and aglycones biochanin, daidzein, and irisolidone. Hg tolerance appeared to be mainly associated to the accumulation of formononetin MalGlc, triclin GlcAGlcA, and afrormosin Glc II in leaves, whereas aglycone accumulation was associated with tolerance to Hg stress in roots. The results evidence the alteration of the flavonoid metabolic profile and their glycosylation processes in response to Hg stress. However, notable differences existed between varieties, both in the basal metabolic profile and in the response to treatment with Hg. Overall, we observed an increase in flavonoid production in response to Hg stress, and Hg tolerance appeared to be associated to a characteristic glycosylation pattern in roots, associated with the accumulation of aglycones and monoglycosylated flavonoids. The findings are discussed in the context of the flavonoid biosynthetic pathway to provide a better understanding of the role of these secondary metabolites in the response and tolerance to Hg stress in *M. truncatula*.

Keywords: *Medicago truncatula*, flavonoids, mercury, metabolomics, heavy metal stress, LC-QTOF

INTRODUCTION

Agricultural soils are increasingly affected by contamination by heavy metals as a consequence of sewage irrigation practices, atmospheric deposition, use of livestock manures, soil amendments, and various agrophytochemicals (Peng et al., 2019). Heavy metals may also be present naturally in soils at low concentrations. However, mines, foundries, and smelters, are the main sources that are often associated with high levels of contamination in soils (Alloway and Alloway, 2013). Plants growing on contaminated soils may accumulate heavy metals in their edible parts, which can result in severe health risks for foraging animals and humans if they enter the food chain (Peralta-Videa et al., 2009; Khan et al., 2015). Heavy metals can disrupt basic metabolic processes, cause displacement of essential metals from biomolecules, and lead to the formation of reactive oxygen species (ROS). Mercury (Hg) is considered the most toxic heavy metal, and Hg contamination is increasing worldwide in both agricultural soils and wild ecosystems. Environmental Hg pollution can be due to natural processes (soil erosion, volcanism, wild fires, and geothermal activities), but is mostly the result of the above-mentioned anthropogenic activities. Bioavailable Hg is readily taken up from the soil and water by different organisms, thus entering the food chain and leading to serious toxicity problems. Mercury has major adverse effects on plants, it creates osmotic stress by competing with necessary nutrients for absorption from the soil, in turn producing a disruption of the plasma membrane. Once inside the cells, Hg has an affinity for sulfhydryl groups and it is capable of binding to enzymes and proteins, replacing essential ions, thereby preventing them from playing their role in the different cellular pathways. In addition, its great capacity to produce cell damage is the formation and accumulation of ROS: superoxides, hydrogen peroxides and hydroxyl radicals (Patra and Sharma, 2000). The molecular mechanisms involved in Hg toxicity and tolerance in plants have been widely investigated (Ortega-Villasante et al., 2005, 2007; Zhou et al., 2007, 2008). A complex cellular defense system involves both enzymatic and non-enzymatic factors in ROS scavenging (Gill and Tuteja, 2010). Antioxidant enzymes superoxide dismutase, catalase ascorbate peroxidase, guaiacol peroxidase, and glutathione-S-transferases constitute the first defense. The non-enzymatic response regulates the production of phytochelatin, polyamines, and metallothioneins, as well as low-molecular weight compounds, such as reduced ascorbic acid, proline, α -tocopherol, glutathione, and different secondary metabolites, including phenolics, carotenoids, and flavonoids (Akram et al., 2017).

Flavonoids make up a very broad group of polyphenolic compounds formed by two aromatic rings (A and B) linked by three carbon atoms that can form another ring C (Panche et al., 2016). They are capable of scavenging ROS because they have hydroxyl groups either in ring A or ring B, which react easily with the free oxygen radicals (Mierziak et al., 2014; Panche et al., 2016). Beside scavenging metal-induced ROS, flavonoids may detoxify metal(oid)s by ion chelation followed by vacuolar sequestration (Ahammed and Yang, 2022). Certain flavonoids are also involved in legume nodule initiation, as reported for

a flavone (7,4'-dihydroxyflavone) and a flavonol (kaempferol) in *Medicago truncatula* (Zhang et al., 2009). Flavonoids are classified into different families that include chalcones, flavanols, flavanones, flavones, flavonols, anthocyanidins, isoflavonoids, and neoflavonoids. This structural variation is combined with a wide variety of decorations that include acylations, hydroxylations, methoxylations, prenylations, or glycosylations (Dixon and Pasinetti, 2010). Glycosides are the most common form of flavonoid derivatives, frequently O-glycosides, and less frequently, C-glycosides (Rauter et al., 2019). Glycosylation may occur with one or multiple sugars units linked to the aglycone moiety in different positions (Harborne and Baxter, 1999). UDP-glycosyltransferases (UGTs) constitute a wide enzyme family and able to glycosylate flavonoids, as well as many other metabolites (Behr et al., 2020). Sugar substitution might modify their antioxidant capacity (Zheng et al., 2017), but also their cellular and tissular location (Taguchi et al., 2000) and it might retroactively regulate their biosynthetic pathways (Zhang and Liu, 2014). Flavonoid aglycones are potentially more antioxidant than their glycosylated forms (Chae et al., 2006), while quercetin and kaempferol glycosylation results in higher ROS scavenging activity (Zhao et al., 2019). Glycosylation of anthocyanins leads to their storage in the vacuole, thus supporting the biosynthesis of these flavonoids *via* feedback inhibition (Li et al., 2017).

Legumes are capable of establishing a symbiotic relationship with certain soil bacteria, collectively known as rhizobia, that leads to the formation of the root nodule, a new organ where bacteria are able to fix atmospheric nitrogen. This symbiotic interaction allows legumes to act as colonizers of degraded soils with little organic matter (Coba de la Peña and Pueyo, 2012). The Rhizobium-legume symbiosis is also considered a potentially powerful tool in the reclamation of polluted soils, due to the pioneer characteristics of legumes and the beneficial effects of the bacteria, which besides making nitrogen fixation possible, have their own detoxifying mechanisms that favor the establishment of the plants (Arregui et al., 2021). Tolerance to stress in legumes needs to consider the symbiotic system, the plant and the bacteria, and can be achieved by cultivar and inoculant selection or by transgenic approaches (Coba de la Peña and Pueyo, 2012). *Medicago truncatula* is a forage legume with high biomass and soil coverage that may represent a suitable pioneer plant in metal-polluted soils, provided that tolerant cultivars are identified, as compatible tolerant rhizobia have been isolated from Hg-contaminated soils (Nonnoi et al., 2012). Moreover, high quality reference genomes and gene annotations (Young et al., 2011; Tang et al., 2014), a HapMap panel of resequenced germplasm (Stanton-Geddes et al., 2013), and a large mutant collection (Lee et al., 2018) are available for this model legume.

In previous studies we were able to identify Hg-tolerant and Hg-sensitive *M. truncatula* cultivars (García de la Torre et al., 2013; Paape et al., 2022) by germplasm screening. As indicated above, the general molecular mechanisms of Hg tolerance and response in plants have been described; however, to our knowledge, the role of flavonoids in the response to Hg stress, has not been investigated. In the present work we aimed to identify the flavonoid profile of Hg-tolerant and Hg-sensitive *M. truncatula* cultivars and to investigate whether

the metabolomic response to Hg stress was related to the level of Hg tolerance. All main subclasses of plant flavonoids are present in the genus *Medicago* (Gholami et al., 2014). Additionally, in a recent genome-wide association study (GWAS) on Hg tolerance in *M. truncatula* (Paape et al., 2022), we identified a UGT gene as a candidate gene within the proximity to the top SNP related to Hg tolerance. Several additional UGT genes were also present in the same region of chromosome 2, and more than 150 UGTs have been identified in the *M. truncatula* genome (Modolo et al., 2007). While the specific substrates of the UGTs nearby the significant SNP are unknown, it is of interest to analyze here the possible role of flavonoid glycosylation in response to Hg stress in *M. truncatula*.

MATERIALS AND METHODS

Plant Material, Plant Growth, and Mercury Treatment

Three Hg-tolerant and one Hg-sensitive cultivar within the HapMap panel were selected according to their seedling relative root growth (RRG), which represents a valid indicator of Hg tolerance in *M. truncatula* (García de la Torre et al., 2013). Tolerant accessions HM081 (RRG = 99.39), HM080 (RRG = 92.00), and HM175 (RRG = 89.96), and sensitive cultivar HM289 (RRG = 21.74) were selected (Paape et al., 2022). Here we will refer to cultivars HM081, HM080, HM175, and HM289 as LR1, LR2, LR3, and LR4, respectively, with L indicating leaves and R indicating roots.

Seeds were obtained from the University of Minnesota, *Medicago* HapMap project (medicagohapmap2.org/germplasm). Seed were scarified with 96% sulfuric acid for 6 min, washed six times with sterile water, further sterilized for 1 min in commercial bleach and washed six times with sterile water, and imbibed in sterile water for 1 h. Seed were germinated in Petri dishes containing agar-water (10 g L^{-1}) for 48 h in the dark at 25°C . Germinated seedlings were inoculated with Hg-tolerant *Ensifer medicae* Amp08 (Nonnoi et al., 2012) by immersion in a fresh bacterial culture ($\text{OD}_{600 \text{ nm}} = 0.8$) for 30 min. Seedlings were then transferred to pots ($6 \text{ cm} \times 6 \text{ cm} \times 8 \text{ cm}$) containing sterile vermiculite and watered with nitrogen-limiting Hoagland nutrient solution [$2.6 \text{ mg L}^{-1} \text{ KNO}_3$, $0.68 \text{ g L}^{-1} \text{ KH}_2\text{PO}_4$, $0.182 \text{ g L}^{-1} \text{ CaCl}_2 \cdot 2\text{H}_2\text{O}$, $0.615 \text{ g L}^{-1} \text{ MgSO}_4 \cdot 7\text{H}_2\text{O}$, $0.109 \text{ g L}^{-1} \text{ K}_2\text{SO}_4$, 0.205 g L^{-1} Hampiron (Rhône Poulenc), and 1.35 mL of a solution containing $11 \text{ g L}^{-1} \text{ H}_3\text{BO}_3$, $6.2 \text{ g L}^{-1} \text{ MnSO}_4 \cdot \text{H}_2\text{O}$, $10 \text{ g L}^{-1} \text{ KCl}$, $1 \text{ g L}^{-1} \text{ ZnSO}_4 \cdot 7\text{H}_2\text{O}$, $1 \text{ g L}^{-1} (\text{NH}_4)_6\text{Mo}_7\text{O}_{24} \cdot 4\text{H}_2\text{O}$, $0.5 \text{ g L}^{-1} \text{ CuSO}_4 \cdot 5\text{H}_2\text{O}$ and $0.5 \text{ mL L}^{-1} \text{ H}_2\text{SO}_4$]. Plants were grown under controlled conditions ($180 \mu\text{mol photon m}^{-2} \text{ s}^{-1}$, $25/20^\circ\text{C}$, 16/8 h photoperiod, 65% relative humidity) for 6 weeks. One set of plants was then treated with mercury using 300 mM HgCl_2 added to the nutrient solution. This treatment did not produce any apparent changes in growth parameters, but led to a significant reduction of nitrogenase activity, which was $\sim 70\%$ of that of control plants. A second set of plants was given no heavy metal treatment and was used as a control group. After 3 days of treatment, roots and leaves were collected separately in Eppendorf tubes containing three sterile 3-mm AISi 304 steel

balls, and tissues were homogenized using a MM400 mixer mill (RETSCH, Haan, Germany). The samples were shaken at a frequency of 30 s^{-1} in six periods of 30 s. To avoid deterioration of the samples during the process, they were immersed in liquid nitrogen between each period. Homogenized samples were frozen in liquid nitrogen and stored at -80°C .

Flavonoid Extraction

The crushed material, approximately 1 g, of leaves and roots of the four target varieties: LR1, LR2, LR3, and LR4, was kept for 12 h in a lyophilizer at a pressure of 0.05 mbar to remove all the moisture. A methanol-water extraction buffer (70–30%) was used, with which a higher concentration of phenolic compounds dissolved in the buffer is achieved (Muñoz et al., 2015). One mL of the extraction buffer was added to 25 mg of lyophilized material reaching a concentration of 25 mg mL^{-1} and placed in the sonicator for half an hour. It was centrifuged for 15 min at 14,800 rpm and 4°C , and the supernatant obtained (containing the extracted flavonoids) was distributed in UHPLC vials.

Liquid Chromatography-Tandem Mass Spectrometry (UPLC- Q-TOF-MS/MS)

An Agilent 1290 UHPLC system coupled to an Agilent 6540 quadrupole time-of-flight mass spectrometer (q-TOF MS) equipped with an orthogonal ESI source was employed for the phytochemical profiling of *M. truncatula* leaves and roots extracts. Chromatographic separation was conducted using a Zorbax Eclipse Plus C18 column ($2.1 \text{ mm} \times 100 \text{ mm}$, $1.8 \mu\text{m}$ particle diameter, Agilent Technologies, Santa Clara, CA, United States) at 30°C . The mobile phase was composed of water (0.1% formic acid, solvent A) and acetonitrile (0.1% formic acid, solvent B). A $5 \mu\text{L}$ aliquot of the sample was injected at a flow rate of 0.5 mL/min during gradient elution. The gradient program was as follows: 0 min, 0% B; 7 min, 30% B; 9 min, 80% B; 11 min, 100% B; 13 min, 100% B; 14 min, 0% B. The mass spectrometer was operated in MS and MS/MS modes for the structural analysis of all compounds. MS parameters were the following: capillary voltage, 4,000 V; nebulizer pressure, 40 psi; drying gas flow rate, 10 L/min ; gas temperature, 350°C ; skimmer voltage, 45 V; fragmentor voltage, 110 V. The MS and Auto MS/MS modes were set to acquire m/z values ranging between 50–1,100 and 50–800, respectively, at a scan rate of 5 spectra per second.

A randomized sequence of samples, including three replicates of each control and treated sample, was analyzed in triplicate. An additional pool of all samples, combining equal aliquots from each sample, was injected regularly throughout the samples sequence, as quality control, to monitor the stability of the analysis. A mix solution of 10 standards, were injected regularly throughout the samples sequence, as second quality control, to validate the LC-HRMS method in terms of retention time and signal variability, and mass accuracy.

Flavonoid Metabolomics Data Analysis

Agilent Mass Hunter Qualitative analysis software version B.07.00 and Agilent Mass Hunter Quantitative (for Q-TOF) analysis software version B.08.00 were used for post-acquisition

data processing. The Molecular Formula Generator algorithm within the Agilent Mass Hunter software was also used to enhance the metabolite database search and mass accuracy calculation (<10 ppm). The accurate mass data, ion source fragmentation, MS/MS fragmentation patterns, MS databases (i.e., NIST, METLIN, and HMDB) and bibliographic search were employed for tentative identification of the phenolic compounds present in the samples.

Both control and Hg-treated samples were submitted to statistical analysis using the online MetaboAnalyst program¹. Univariate analysis based on *T*-test and Fold change (FC) analysis was applied to detect differentially accumulated flavonoids (*p*-value cut-off: 0.05) with a defined absolute value of change (FC > 2.5) between control and treated samples. To improve data interpretation, multivariate data analysis based on a cluster heatmap hierarchical clustering and principal component analysis (PCA) was carried out. Hierarchical clustering was applied using a complete linkage clustering method with Pearson distance measurement. PCA was carried out using the statistical software The Unscrambler V9.7 (CAMO Software AS, Oslo, Norway). Multivariate data matrix was analyzed after data autoscaling (data were mean-centered and divided by the standard deviation of each variable).

RESULTS

Flavonoids Metabolomics Analysis of *Medicago truncatula* Cultivars With Different Degree of Hg Tolerance

Leaves and roots of the selected *M. truncatula* varieties grown under control conditions were subjected to an extensive flavonoid profiling analysis to evaluate their accumulation profiles. Full-scan HRMS data obtained in ESI(+) ionization mode were screened for expected polyphenols reported in *M. truncatula* (Jasiński et al., 2009; Marczak et al., 2010; Staszko et al., 2011; Gholami et al., 2014). This targeted approach allowed chromatographic peak detection of suspected flavonoids, on the basis of accurate mass and isotopic distribution. Further structural information was obtained from HRMS/MS data acquired by data-dependent scan in auto MS/MS mode. Diagnostic product ions and neutral loss filtering of MSMS data were applied to screen for structurally related flavonoids, including isomers and glycoconjugate derivatives with different substitution patterns on the aglycone.

Following the proposed profiling strategy, the analyzed extracts of *M. truncatula* revealed the presence of at least 46 phenolic compounds, classified into five different flavonoid families: three anthocyanidins (1, 12, 21), 26 flavones (2, 4–10, 13–16, 18–20, 22–28, 30, 34, 35, 40), 14 isoflavones (3, 11, 17, 29, 31–33, 38, 39, 42–46), two pterocarpan flavonoids (37, 41), and one flavanone (36; Table 1).

Most of the compounds detected were conjugated flavonoids, derivatives of apigenin, tricetin, chrysoeriol, biochanin, afrormosin, formononetin, and peonidin, mainly glycosylated

with glucose and/or glucuronic acid molecules. Some of these compounds were also acylated with ferulic, coumaric, or malonic acid. Sugar moieties (e.g., GlcA-glucuronic acid, Glc-glucose) and acyl groups on sugar rings (e.g., Fer-ferrulic acid, Cou-Coumaric acid, Mal-malonic acid) were annotated based on characteristic neutral losses and product ions (Figure 1). Thus, the CID-MS/MS (collision-induced dissociation tandem mass spectrometry) pattern of flavonoid glycosides was mainly characterized by the cleavages of consecutive glycosidic bonds, either between glucoside or glucuronic acid molecules, or between sugar and the flavone moieties (Figure 1A). However, the CID-MS/MS spectra of acylated glycoconjugates showed product ions with charge retained on glucuronic acid moieties acylated with ferulic (Figure 1B) or coumaric acid (Figure 1C).

Substantial differences in flavonoid accumulation were observed among leaves and roots for the studied *M. truncatula* varieties. The abundance of total flavonoids in leaf samples was remarkably higher than in roots; accounting for a total content between 4.6- and 16.0-fold higher (Figure 2A). Thus, an increase in flavonoid's accumulation ratio between leaves and roots could be observed: L/R1 (4.6) < L/R2 (7.0) < L/R3 (7.2) << L/R4 (16), as Hg-tolerance decreases (LR1 > LR2 > LR3 >> LR4). Figure 2B displays the relative abundance of different flavonoid families in *M. truncatula* leaves and roots for the target varieties. The heatmap reveals higher levels of tricetin-, apigenin-, and chrysoeriol-type flavones, as well as peonidin-type anthocyanidins in leaf samples, whereas higher concentrations of daidzein-, biochanin A-, irisolidone-, and formononetin-type isoflavones were found in roots.

Leaves contained mainly tricetin and apigenin glycoconjugates, accounting for a total contribution ranging from 81 to 93% of total flavonoids (Figure 3 and Supplementary Table 1). Hg-tolerant variables (LR1, LR2, and LR3) accumulate tricetin-type flavones (48–81%) as major compounds, whereas the most Hg-sensitive variable (LR4) accumulates mainly apigenin-type flavones (66%) in leaf samples. Unlike the aerial part, roots contained mainly formononetin-type isoflavones (77–88%).

A comparative flavonoid profiling analysis of the target varieties can be observed in the heatmap of Figure 4, showing a color code from high to low concentration ranging from dark red to dark blue. Leaves and root samples were grouped according to their flavonoid content based on a cluster analysis (Figure 4). Most of flavonoids detected in leaves are glycoconjugated derivatives containing from 1 to 3 sugar units (glucose or glucuronic acid; Figure 5A). The accumulation levels of free aglycones in leaves is below 3% of the total flavonoids content. Apigenin mono- and diglucuronide (16, 5), as well as a set of positional isomers of apigenin di- and triglucuronides acylated with ferulic (9, 15, 19, 22, 26) or coumaric (10, 18, 20, 30) acids are highly abundant in LR4, followed by LR2, LR1, and LR3. Another major group of flavones in leaf samples involve tricetin monoglucosides (14, 24, 28, 40), glucuronyl-glucosides (2, 4, 8), diglucuronides (7), feruloyl-diglucuronides (25, 35), and coumaroyl-diglucuronides (27, 34). The accumulation of these tricetin glycosides is higher in Hg-resistant varieties than in the Hg-sensitive cultivar. Wider accumulation variability for the different varieties was observed for chrysoeriol mono- and

¹www.metaboanalyst.ca

TABLE 1 | Tentatively identified flavonoids and their glycoconjugates from *Medicago truncatula* roots and leaves by ESI(+)-q-TOF-MS/MS analysis, including the retention time (min), molecular formula, experimental molecular ions, calculated mass error ($\Delta m/z$, ppm), and MS/MS product ions.

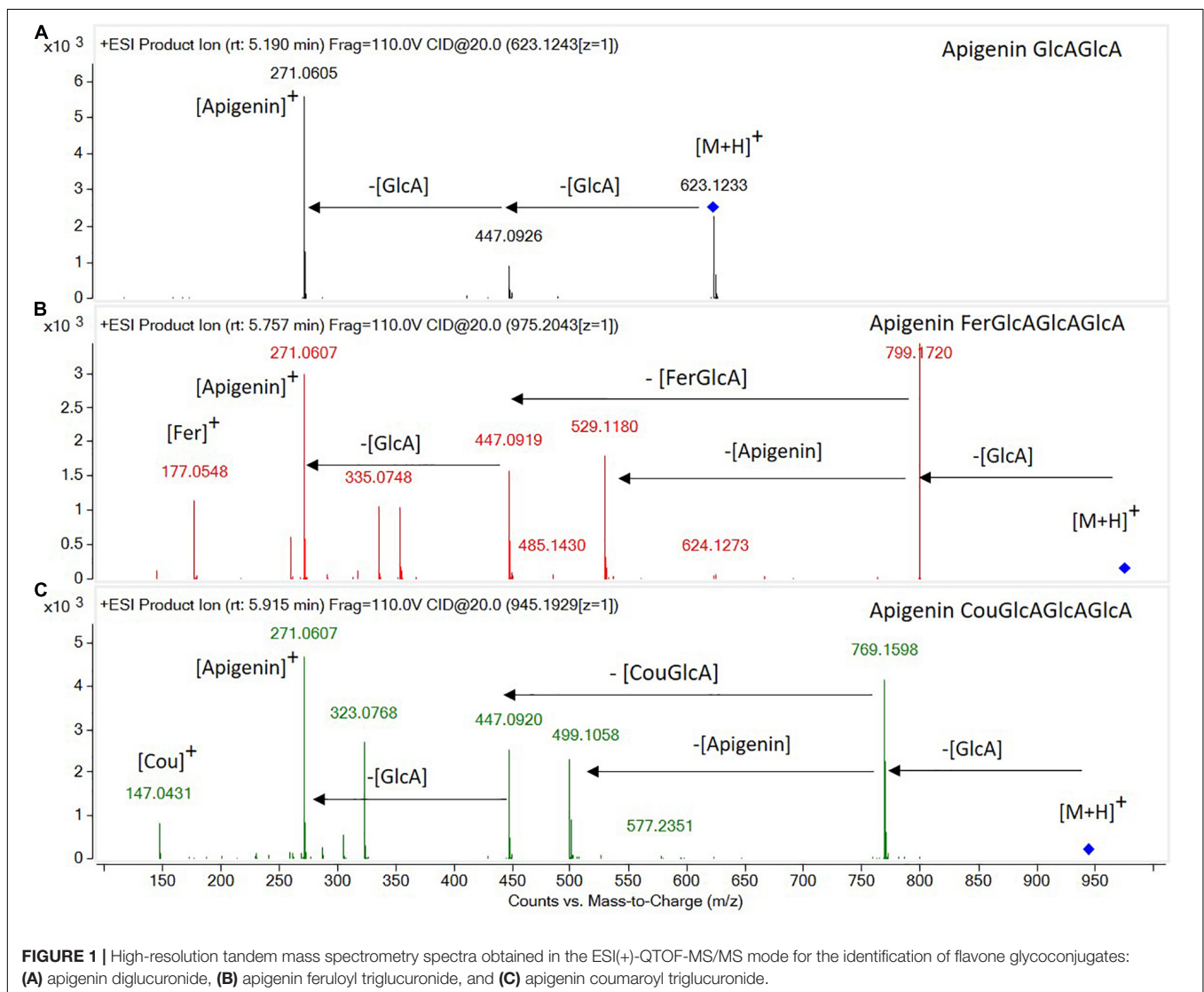
Peak no	Ret. time (min)	Family	Key	Tentative identification	Formula	Monoisotopic mass	m/z [M+H] ⁺ (theoretical)	Error (ppm)	MS/MS product ions (m/z)
1	4.60	Anthocyanidin	Peon-G01	Peonidin Glc I	C22H23O11+	463.1240	463.1240	1.8	301.0702
2	4.61	Flavone	Tric-G01	Tricin GlcGlcA I	C29H32O18	668.1589	669.1662	0.3	507.1119, 331.0817
3	5.07	isoFlavone	Afror-G01	Afrormosin Glc I	C23H24O10	460.1369	461.1442	-0.4	461.1418, 299.0905
4	5.13	Flavone	Tric-G02	Tricin GlcGlcA II	C29H32O18	668.1584	669.1657	-0.2	507.1119, 331.0817
5	5.18	Flavone	Api-G01	Apigenin GlcAGlcA	C27H26O17	622.1170	623.1243	-0.2	271.0592
6	5.39	Flavone	Chry-G01	Chrysoeriol GlcAGlcA	C28H28O18	652.1280	653.1353	0.9	477.1025, 301.0709
7	5.49	Flavone	Tric-G03	Tricin GlcAGlcA	C29H30O19	682.1387	683.1460	1.4	507.1119, 331.0817
8	5.77	Flavone	Tric-G04	Tricin GlcGlcA III	C29H32O18	668.1590	669.1663	0.0	507.1119, 331.0817
9	5.81	Flavone	Api-G02	Apigenin FerGlcAGlcAGlcA I	C43H42O26	974.1975	975.2048	-0.2	799.1716, 447.0922, 323.0769, 271.0598
10	5.90	Flavone	Api-G04	Apigenin CouGlcAGlcAGlcA I	C42H40O25	944.1865	945.1938	-0.2	769.1589, 447.0922, 323.0769, 271.0598
11	5.93	isoFlavone	Form-G01	Formononetin Glc I	C22H22O9	430.1264	431.1337	0.9	269.0798
12	5.96	Anthocyanidin	Peon-G02	Peonidin Glc II	C22H23O11+	463.1240	463.1240	1.8	301.0702
13	5.97	Flavone	Chry-G02	Chrysoeriol FerGlcAGlcAGlcA	C44H44O27	1,004.2073	1,005.2146	-0.1	477.1025, 301.0709
14	6.03	Flavone	Tric-G05	Tricin Glc I	C23H24O12	492.1268	493.1341	-2.1	331.0817
15	6.08	Flavone	Api-G05	Apigenin FerGlcAGlcAGlcA II	C43H42O26	974.1970	975.2043	-0.2	799.1716, 447.0922, 323.0769, 271.0598
16	6.19	Flavone	Api-G03	Apigenin GlcA	C21H18O11	446.0849	447.0922	-0.9	271.0587
17	6.29	isoFlavone	Bioch-G01	Biochanin A MalGlc I	C25H24O13	532.1217	533.1290	1.8	285.0762
18	6.30	Flavone	Api-G07	Apigenin CouGlcAGlcAGlcA II	C42H40O25	944.1865	945.1938	-0.2	769.1589, 447.0922, 323.0769, 271.0598
19	6.32	Flavone	Api-G06	Apigenin FerGlcAGlcA I	C37H34O20	798.1643	799.1716	-1.1	447.0926, 271.0601, 353.0876
20	6.36	Flavone	Api-G08	Apigenin CouGlcAGlcA I	C36H32O19	768.1538	769.1611	-0.8	447.0922, 323.0769, 271.0598
21	6.40	Anthocyanidin	Peon-G03	Peonidin Glc III	C22H23O11+	463.1240	463.1240	1.8	301.0702
22	6.40	Flavone	Api-G09	Apigenin FerGlcAGlcAGlcA III	C43H42O26	974.1965	975.2038	0.1	799.1716, 447.0922, 323.0769, 271.0598
23	6.41	Flavone	Chry-G03	Chrysoeriol GlcA	C22H20O12	476.0955	477.1028	-1.5	477.1025, 353.0553, 301.0709
24	6.48	Flavone	Tric-G06	Tricin Glc II	C23H24O12	492.1268	493.1341	-2.1	331.0817
25	6.53	Flavone	Tric-G07	Tricin FerGlcAGlcA I	C39H38O22	858.1855	859.1928	-0.3	507.1119, 331.0817
26	6.58	Flavone	Api-G10	Apigenin FerGlcAGlcA II	C37H34O20	798.1643	799.1716	-0.6	447.0920, 271.0607, 353.0876
27	6.61	Flavone	Tric-G08	Tricin CouGlcAGlcA I	C38H36O21	828.1727	829.1800	-0.6	507.1119, 331.0817
28	6.72	Flavone	Tric-G09	Tricin Glc III	C23H24O12	492.1268	493.1341	-2.1	331.0817
29	6.83	isoFlavone	Form-G02	Formononetin Glc II	C22H22O9	430.1264	431.1337	0.9	269.0798
30	6.92	Flavone	Api-G11	Apigenin CouGlcAGlcA II	C36H32O19	768.1538	769.1611	-0.9	447.0922, 323.0769, 271.0598
31	6.94	isoFlavone	Daiz	Daidzein	C15H10O4	254.0579	255.0652	-1.6	255.0649
32	6.95	isoFlavone	Bioch-G02	Biochanin A MalGlc II	C25H24O13	532.1217	533.1290	0.5	285.0762
33	6.97	isoFlavone	Afror-G02	Afrormosin Glc II	C23H24O10	460.1369	461.1442	-2.8	461.1418, 299.0905
34	7.06	Flavone	Tric-G10	Tricin CouGlcAGlcA II	C38H36O21	828.1727	829.1800	-2.8	507.1119, 331.0817
35	7.19	Flavone	Tric-G11	Tricin FerGlcAGlcA III	C39H38O22	858.1855	859.1928	0.8	507.1119, 331.0817
36	7.29	Flavanone	Narin-G	Naringenin Chalcone Glc	C21H22O10	434.1213	435.1286	-0.7	391.1364, 271.0432
37	7.60	Pterocarpan	Medi-G01	Medicarpin MalGlc I	C25H26O12	518.1424	519.1497	-1.0	271.0964
38	7.67	isoFlavone	Form-G03	Formononetin MalGlc	C25H24O12	516.1268	517.1341	-1.5	269.0798
39	7.71	isoFlavone	Afror-G03	Afrormosin MalGlc	C26H26O13	546.1373	547.1446	-0.4	547.1444, 299.0907
40	8.07	Flavone	Tric-G12	Tricin Glc IV	C23H24O12	492.1268	493.1341	-2.1	331.0817
41	8.15	Pterocarpan	Medi-G02	Medicarpin MalGlc II	C25H26O12	518.1424	519.1497	-1.0	271.0964

(Continued)

TABLE 1 | (Continued)

Peak no	Ret. time (min)	Family	Key	Tentative identification	Formula	Monoisotopic mass	m/z [M+H] ⁺ (theoretical)	Error (ppm)	MS/MS product ions (m/z)
42	8.24	isoFlavone	BiochA	Biochanin A	C ₁₆ H ₁₂ O ₅	284.0684	285.0757	-1.4	285.0757
43	8.39	isoFlavone	Iriso-Iso	Irisolidone isomer	C ₁₇ H ₁₄ O ₆	314.0790	315.0863	-3.4	315.0863
44	8.56	isoFlavone	Form	Formononetin	C ₁₆ H ₁₂ O ₄	268.0735	269.0808	-2.6	269.0806
45	8.64	isoFlavone	Afror	Afrormosin	C ₁₇ H ₁₂ O ₅	298.0841	299.0914	-1.3	299.0902
46	9.11	isoFlavone	Iriso	Irisolidone	C ₁₇ H ₁₄ O ₆	314.0790	315.0863	-3.1	315.0863

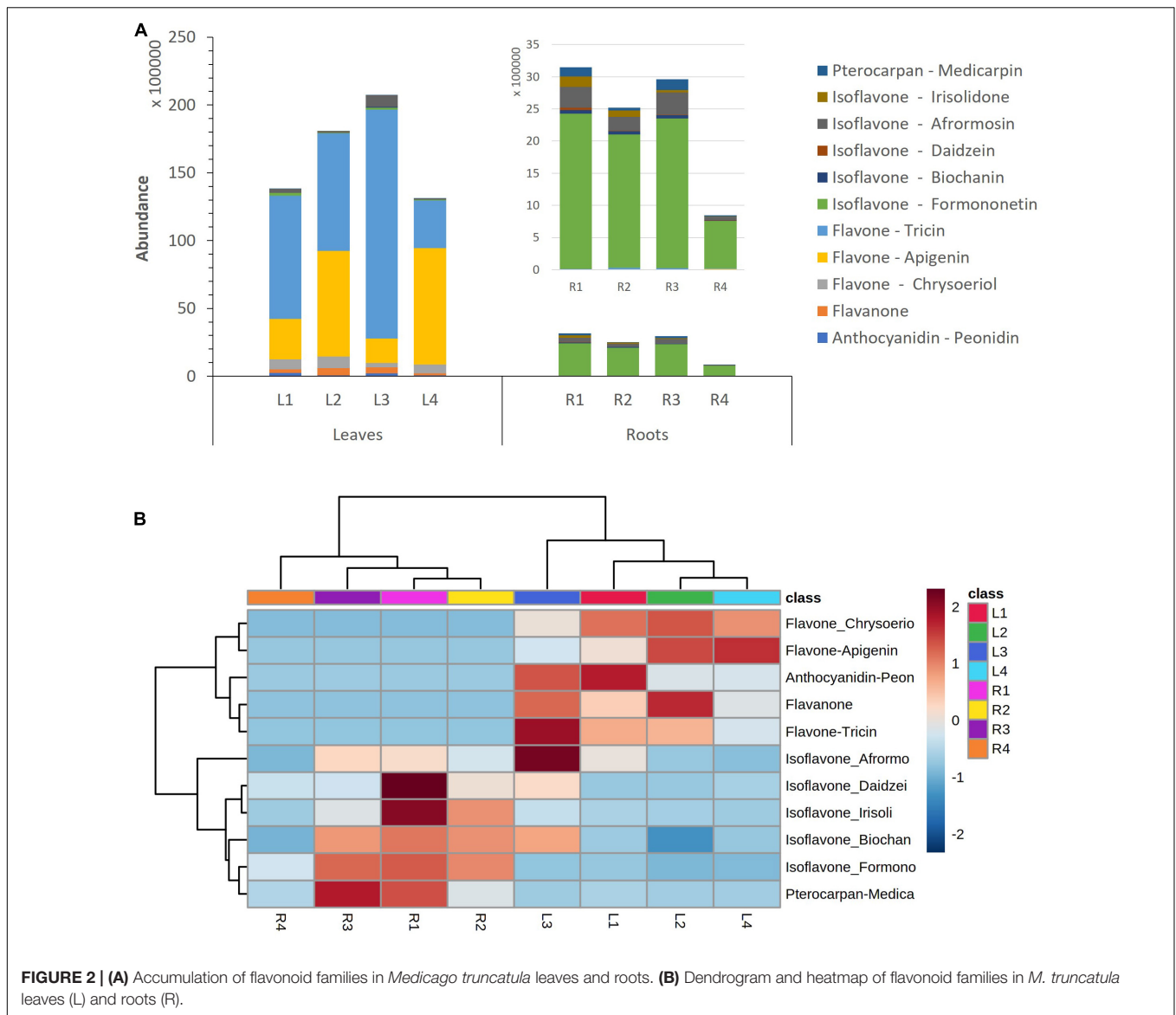
Abbreviations of sugars and acyl groups: GlcA, glucuronic acid; Glc, glucose; Mal, malonic acid; Fer, ferulic acid; and Cou, Coumaric acid.



diglucuronide (23, 6), chrysoeriol feruloyl-triglucuronide (13) and the three positional isomers of the anthocyanidin peonidin glucoside (1, 12, 21).

Flavonoid aglycones are considered more antioxidant than their glycosylated forms (Chae et al., 2006). The detected levels of free aglycones in roots are between 36 and 77%, depending on the variety (Figure 5A), and the conjugated derivatives were mainly monoglucosylated and malonylated flavonoids. Free isoflavones

such as biochanin A (42), formononetin (44), irisolidone (43, 46), and daidzein (31) were highly enriched in root samples. The levels of glucosylated and malonylglucosylated derivatives of medicarpin (37, 41) and its isoflavone precursors formononetin glucoside and malonylglucoside (29, 38), as well afrormosin glucoside (3) and biochanin A malonylglucoside (32), were mainly present in Hg-tolerant root samples. According to the flavonoid profiling analysis carried out in control samples of



leaves and root tissues, the synthesis of free isoflavones, followed by monoglycosylation and further malonylation was shown to be more characteristic of roots samples, whereas a higher glycosylation degree (di- and triglycosides), followed by further acylation with coumaric and ferulic acid were more characteristic of leaf tissues.

Differential Flavonoid Accumulation in *Medicago truncatula* Cultivars in Response to Hg Stress

Despite the observed differences in flavonoid profiles among the target *M. truncatula* varieties and among leaves and roots samples, the results obtained after Hg-treatment suggest flavonoid accumulation changes of different magnitude, according to the tissue sample (leaves or roots). Total flavonoid accumulation and glycosylation profiles for control and

Hg-treated samples are comparatively displayed in **Figures 5B,C**, whereas the effects of Hg stress on individual flavonoid profiles are shown in **Figure 6**. A set of differentially expressed metabolites, exhibiting accumulation values with $FC > 2.5$ (upregulated: $\text{Log}_2 FC > 1.3$) or $FC < 0.4$ (downregulated: $\text{Log}_2 FC < -1.3$) in Hg-treated compared to control samples, is summarized in **Table 2**.

Total flavonoid accumulation results in leaf samples (**Figure 5B**) showed slight changes in some varieties (L1 and L2) after they were Hg-treated, although in general no significant variations were observed either in the flavonoid profile or in the glycosylation degree. Comparing the expression profile of individual flavonoids in control and Hg-treated varieties (**Figure 6**), similar flavonoid accumulation patterns could be observed in general, except for some particular metabolites. Thus, the monoglycosylated and malonylated derivatives of peonidin (Peon-G01), medicarpin (Medi-G02), were strongly

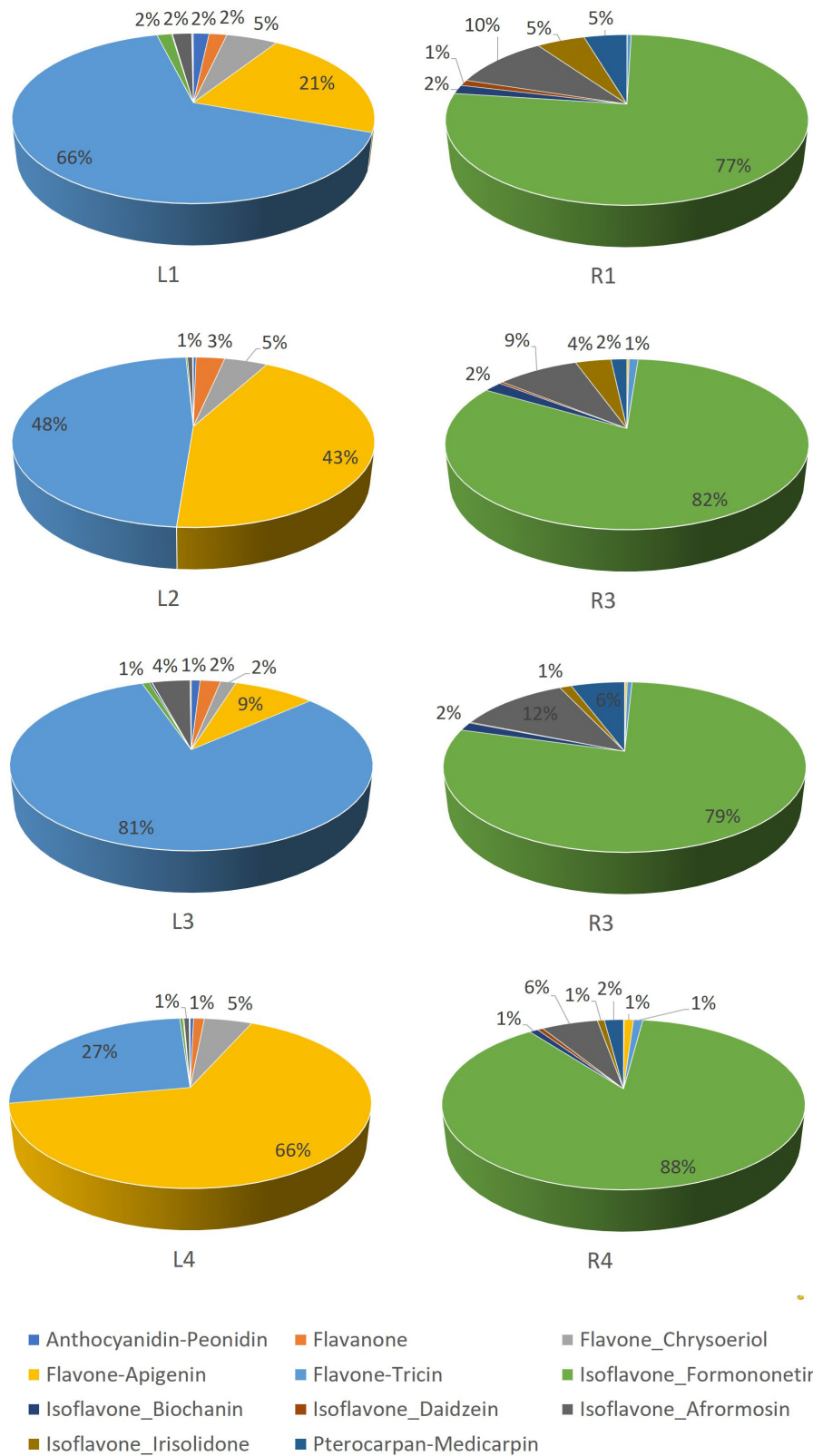


FIGURE 3 | Relative abundance (%) of flavonoid families in *Medicago truncatula* leaves and roots.

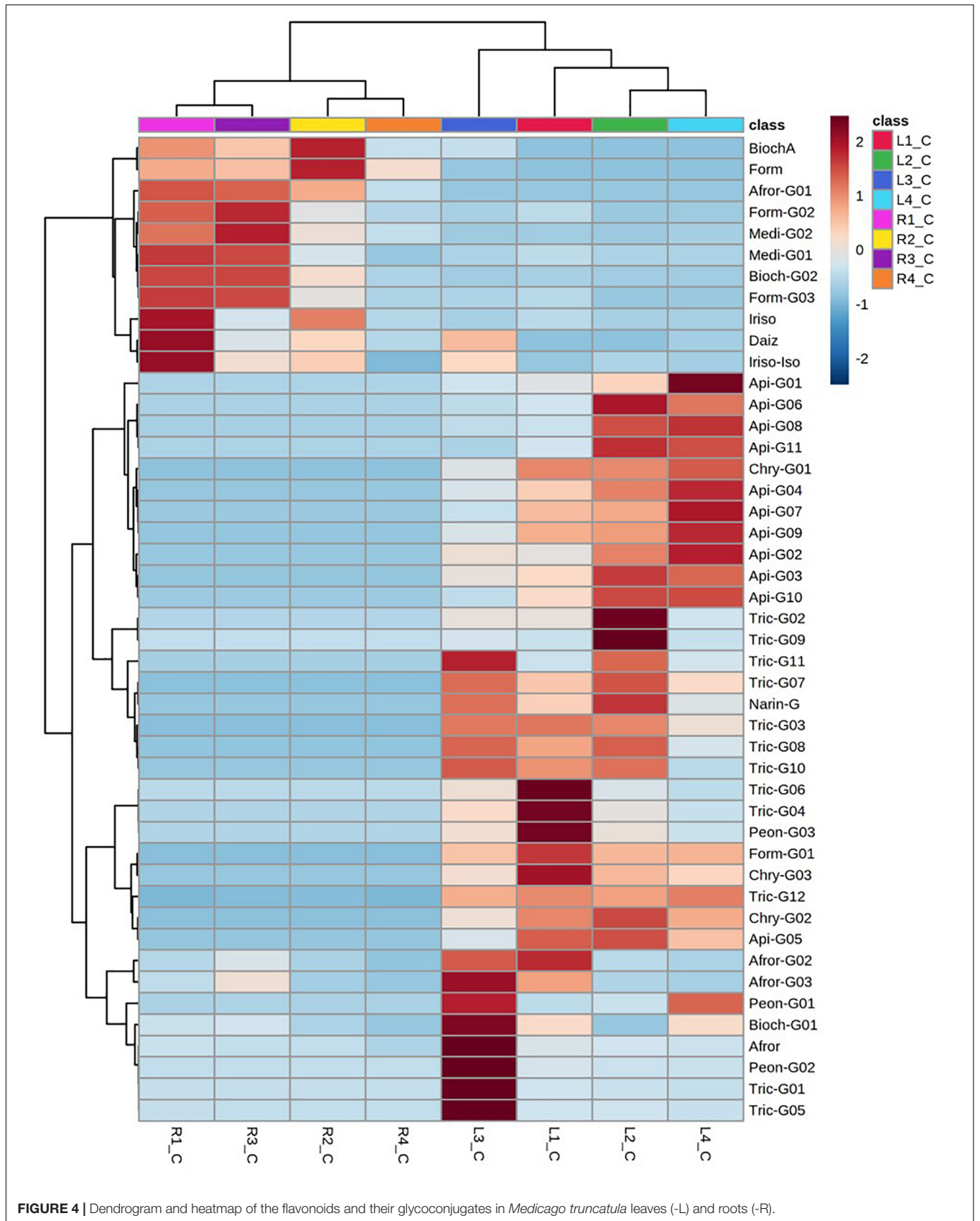
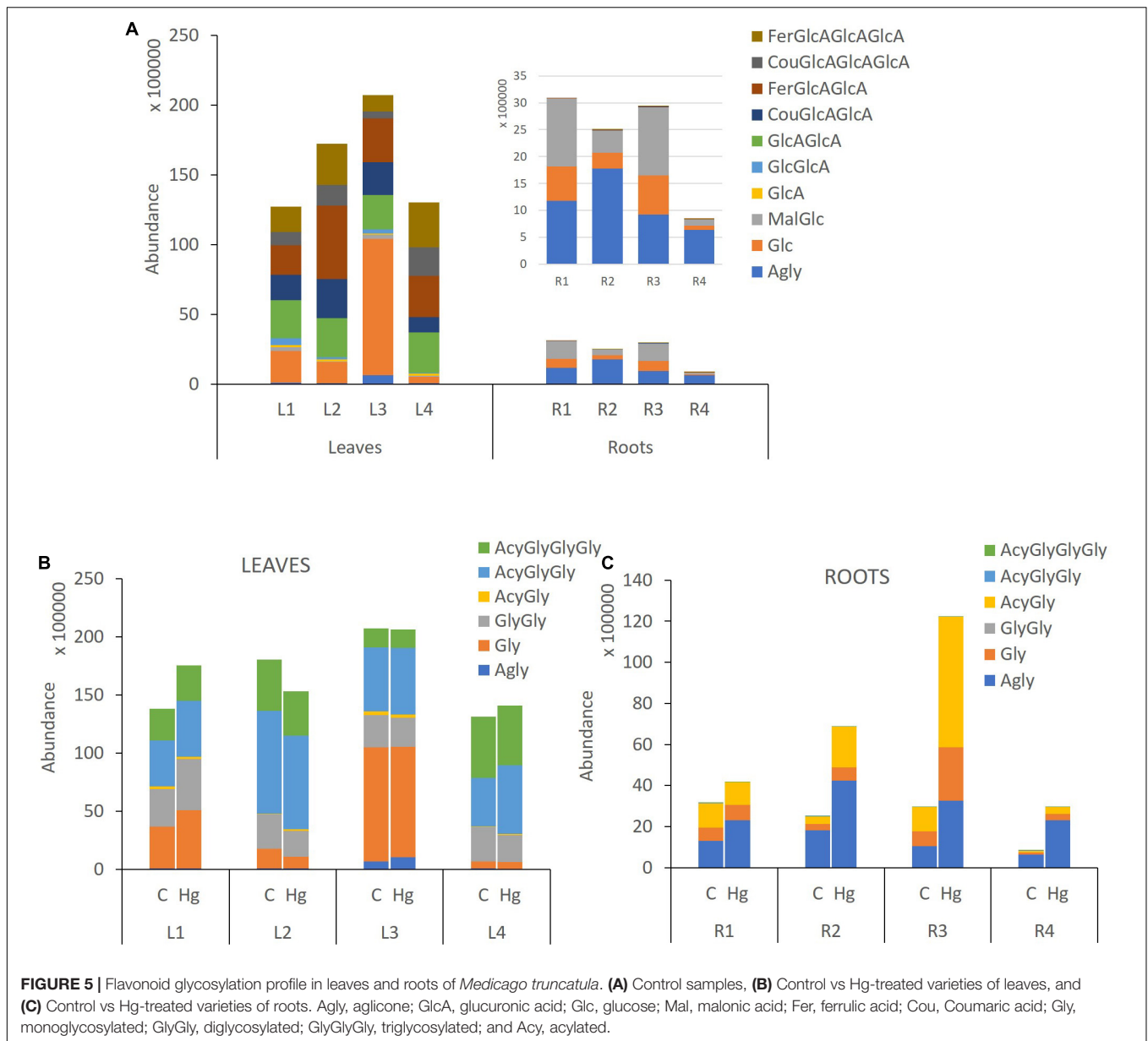


FIGURE 4 | Dendrogram and heatmap of the flavonoids and their glycoconjugates in *Medicago truncatula* leaves (-L) and roots (-R).

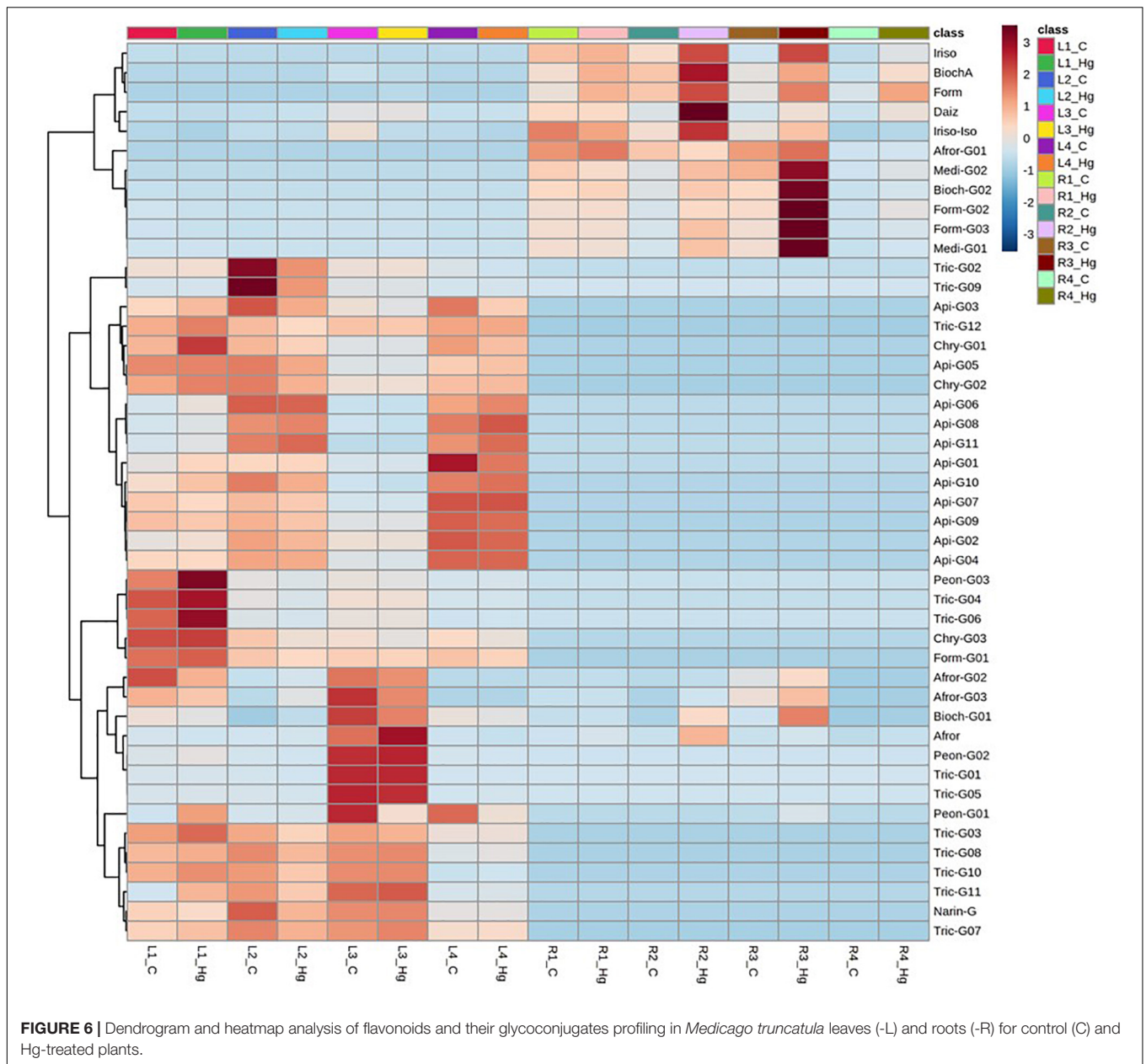


deregulated metabolites in L1, L3, and L4 varieties, whereas malonylglucosides of biochanin A (Bioch-G02 and Bioch-G01) and formononetin (Form-G02 and Form-G03) were mainly deregulated in L1 and L2 under Hg stress. This behavior suggests that treatment with Hg does not cause generalized alterations with respect to the basal state, but rather punctual alterations in the synthesis of specific flavonoids in leaves.

Unlike leaf samples, significant quantitative changes could be observed in the accumulation of a wider range of flavonoids and their conjugate derivatives in roots, as a result of the Hg treatment. As displayed in **Figure 5C**, the stress caused by Hg caused a significant increase in both the levels of free and glycosylated flavonoids. The most abundant aglycone in roots, formononetin, exhibited increasing FC values: R1 (1.8) > R2 (2.3) > R3 (3.1) > R4 (3.6), as Hg-tolerance decreases. A similar trend was

shown for formononetin monoglycoside R1 (1.1) > R2 (2.1) > R3 (3.6) > R4 (3.8). The expression profile of individual flavonoids in roots under Hg stress was notably more altered compared to leaf flavonoids profile under the same conditions, as clearly observed in **Figure 6**. Eight flavonoids were strongly upregulated in three of the target root varieties, involving malonylglucosides of biochanin A (Bioch-G01, Bioch-G02), formononetin (Form-G03), and medicarpin (Medi-G01), followed by the aglycones biochanin, daidzein, and irisolidone.

The results presented above evidence the alteration of the flavonoids metabolic profile and their glycosylation processes in response to Hg stress. However, notable differences have been seen between varieties, both in the basal metabolic profile and in the response to treatment with Hg. In order to explore patterns of metabolic response (flavonoid accumulation) to



Hg stress as a function of the tolerance of each variety, a multivariate data analysis was carried out. For this purpose, flavonoid compounds identified in the targeted profiling analysis along with the Hg-tolerance values obtained for each variety of *M. truncatula* were jointly evaluated through a PCA. The proposed unsupervised multivariate analysis tool allows the evaluation of the compositional variability of the data in order to obtain the correlation structure between flavonoids accumulation and Hg tolerance values for the target varieties. Associations between variables were established by proximity in the multivariate space. Two PCA were carried out to evaluate the possible associations between individual flavonoids (Figure 7), and flavonoid glycosylation degree (Figure 8), with the Hg-tolerance of the studied varieties.

According to the PCA results, graphically displayed in Figure 7, the first two principal components (PC1, PC2) explained the 72 and 71% of the total variance for leaves and roots, respectively. In both tissue samples, a trend from lower to higher Hg-tolerance is observed along the positive direction of PC1 components that explains 45% (PC1-A) and 50% (PC1-B) of the total variance. As can be clearly observed in Figure 7A, control and treated leaf samples of each variety are located close to each other in the multivariate space, suggesting that the variability between varieties is greater than the variability caused by the treatment. This behavior suggests that the treatment with Hg does not cause greater differences in the accumulation of leaf flavonoids than those due to the differences between varieties in basal state. Leaf samples distributed in the positive side of

TABLE 2 | Differentially accumulated flavonoids ($\text{Log}_2 \text{FC}$) in *Medicago truncatula* varieties after Hg-treatment.

COMPOUND NAME	LEAVES				ROOTS			
	L1	L2	L3	L4	R1	R2	R3	R4
Afromosin						3.3		2.3
Afromosin Glc I								3.3
Afromosin MalGlc		1.4				1.6		
Apigenin GlcAGlcA					2.4			
Apigenin FerGlcAGlcAGlcA I						-3.7	-1.6	
Apigenin CouGlcAGlcAGlcA I						-3.6	3.8	
Apigenin FerGlcAGlcAGlcA II								-2.1
Biochanin A MalGlc I		4.5				2.7	2.2	2.2
Biochanin A MalGlc II	-2.1					1.7	2.1	1.8
Biochanin A						1.3	1.4	1.9
Daidzein	-2.6	1.9				3.4	1.6	2.3
Formononetin			2.1				1.6	1.8
Formononetin Glc II	-1.4	2.4					2.3	2.6
Formononetin MalGlc	-1.4	3.3				2.4	2.5	1.8
Irisolidone						1.6	3.7	2.9
Irisolidone isomer	-1.6		-1.6			1.6		1.3
Medicarpin MalGlc I						2.5	2.4	1.9
Medicarpin MalGlc II	-2.6		-2.4	-4.1		1.5		
Peonidin Glc I	2.9		-1.8	-1.6				
Tricin GlcAGlcA						-3.3		1.4
Tricin Glc I							3.1	
Tricin FerGlcAGlcA I						-3.1		
Tricin CouGlcAGlcA I					-3.1	-4.8		
Tricin FerGlcAGlcA III	2.2							

Upregulated: $\text{Log}_2 \text{FC} > 1.33$ (red); Downregulated: $\text{Log}_2 \text{FC} < 1.33$ (green).

5 2 0 -2 -5

PC1 axis (L1 and L3) were associated with tolerance, whereas the sample with the most negative contribution on the PC1 axis (L4) is associated with the lowest tolerance.

In roots (**Figure 7B**), greater differences were observed in the accumulation of flavonoids in response to Hg stress. Tolerant cultivars under Hg-treatment (R1-Hg, R2-Hg, and R3-Hg) present a positive contribution in the PC1 axis, located in the tolerance zone where the Hg tolerance variable exhibit higher weight. On the contrary, both control and treated root samples of the less tolerant variety (R4-C and R4-Hg) showed strong negative contributions in PC1. Although R1, R2, and R3 are tolerant samples, their response to Hg-treatment was shown to be different in terms of flavonoids accumulation. This behavior might be explained due to their differences in the basal profile of flavonoids. Thus, R1-Hg is slightly displaced from R1-C sample, both located in positive PC1 component, indicating similar flavonoids accumulation in the basal state and under Hg stress conditions. However, R2-Hg and R3-Hg undergo a more pronounced displacement from their basal state (R2-C and R3-C in the negative PC1) toward positive contributions in the tolerance zone. This behavior evidences deeper changes in the flavonoids metabolic profile of R2 and R3 samples that allow them to tolerate Hg-stress, whereas R1 undergo slight modifications in response to Hg stress. The loading plot (**Supplementary Figure 1**) suggest

that Hg-Tolerance might be associated to the accumulation of formononetin MalGlc (Form-G03), triclin GlcAGlcA (Tric-G03), and afromosin Glc II (Afror-G02), among others, in leave samples, whereas the aglycones such as afromosin, baidzein, biochanin A, and formononetin are associated with tolerance to Hg stress in root samples.

Another multivariate data analysis was also carried out based on the flavonoids glycosylation degree of the target control and Hg-treated varieties. The resulting PCA bi-plots are graphically displayed in **Figure 8**, where the first two principal components (PC1, PC2) explained the 78 and 69% of the total variance for leaves and roots, respectively. Sample grouping and distribution in the multivariate space showed similarities with the previous analysis based on the individual flavonoids profile. While control and treated leave samples of each variety grouped together, greater differences were observed between control and Hg-treated roots samples. Since the variability between varieties is greater for leaves than the variability caused by the treatment, no association could be done between flavonoids glycosylation and Hg-stress. However, a trend from lower to higher Hg-tolerance was observed along the positive direction of PC1 components that explains 57% (PC1-A) of the variability (**Figure 8A**). Tolerant L1 and L3 varieties were placed on the positive side of PC1, whereas the less tolerant L4 variety exhibited the most negative contribution

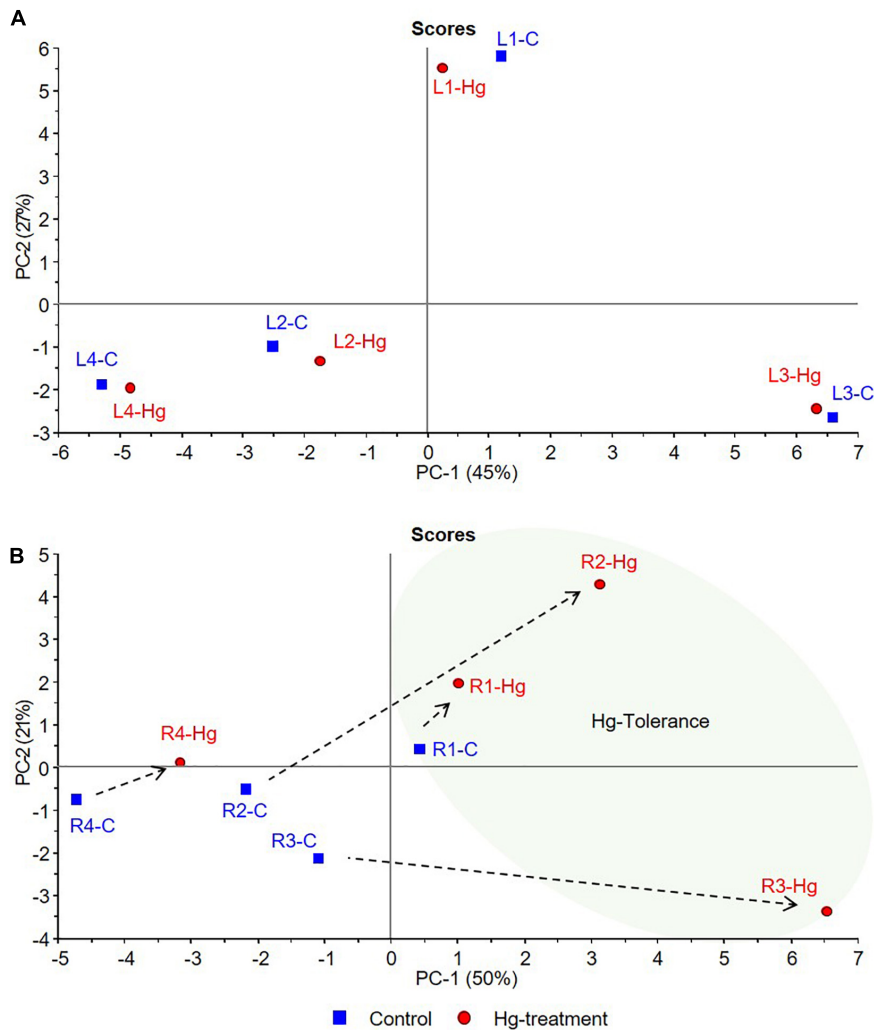


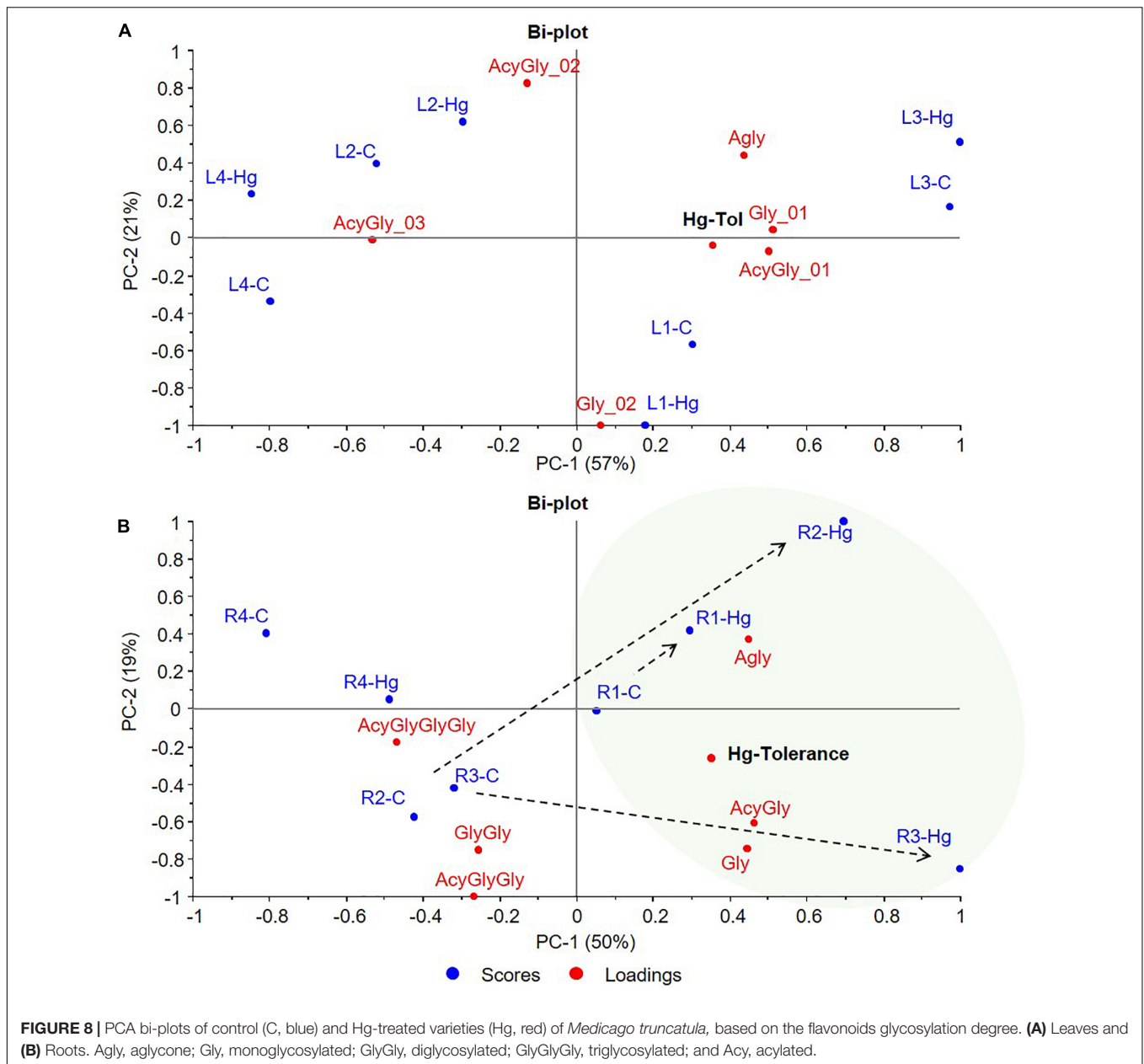
FIGURE 7 | PCA score plots of control (C, blue) and Hg-treated varieties (Hg, red) of *Medicago truncatula*, based on individual flavonoid accumulation. **(A)** Leaves and **(B)** Roots.

in PC1. This trend is even more clear in **Figure 8B**, where Hg-treated roots (R1-Hg, R2-Hg, and R3-Hg) shifted with respect to the untreated controls toward the positive side of PC1, that is, the tolerance zone. Thus, under Hg stress, Hg-tolerant root samples showed a characteristic glycosylation pattern with positive contributions in the tolerance zone, which seems to be more associated with the accumulation of aglycones and low-glycosylated flavonoids (monoglycosylated) with higher contribution in positive PC1.

DISCUSSION

Several profiling studies, mainly based on HPLC-MS/MS methods have investigated the flavonoid components of *M. truncatula* (Jasiński et al., 2009; Marczak et al., 2010; Staszaków et al., 2011). GC-MS was also employed after enzymatic hydrolysis of conjugate flavonoids to assign the sugar

stereochemical configuration (Farag et al., 2007; Schliemann et al., 2008). Complementary spectroscopic techniques, including UV and nuclear magnetic resonance (NMR) detectors were also used to accurately elucidate their structures, increasing the number of identified flavonoid components (Kowalska et al., 2007; Jasiński et al., 2009). These advances allowed the investigation of the changes in the profile of flavonoid accumulation in *M. truncatula* under biotic stress (Jasiński et al., 2009), among others. The CID-MS/MS allowed us to define a pattern of flavonoid glycosides that was mainly characterized by the cleavages of consecutive glycosidic bonds or between sugar and the flavone moieties. We also identified product ions with charge retained on glucuronic acid moieties acylated with ferulic or coumaric acid. This typical fragmentation suggests O-glycosidic bonding (Jasiński et al., 2009), whereas the position of sugar acylation, as well as those of glycosidic bonds between the aglycone and sugar or sugars have been reported in LC/MS-based structural elucidation works, where



NMR spectra have been included (Kowalska et al., 2007; Jasiński et al., 2009). In leaves, our results are in line with previous works, reporting contents of flavone glycoconjugates in relative concentrations greatly exceeding those of isoflavones in *M. truncatula* leaves (Jasiński et al., 2009). The prevalence of glycoconjugates substituted with glucuronic acid moieties that we observed related to aglycones is supported by earlier studies performed on leaves from *M. truncatula* (Staszów et al., 2011). The presence of a higher concentration of isoflavone derivatives in root tissues is most probably due to the fact that intense interactions with other organisms, mainly rhizobia, but also other bacteria, fungi, insects, and other plants occur in the rhizosphere. Many plant species use isoflavonoids as signaling and defense compounds in their interactions

with both symbionts and pathogenic microbes. In addition, roots of leguminous plants exude specific flavonoids into the rhizosphere, which act as chemical attractants for symbiotic nitrogen-fixing bacteria (Oldroyd et al., 2005; Jasiński et al., 2009).

The role of flavonoids in the response to heavy metals, specifically mercury, has not been investigated to date. To the best of our knowledge, the present study is the first metabolomic analysis of *M. truncatula* focused on flavonoids accumulation in response to mercury stress.

Under environmental stresses, plant cells initiate gene expression programs at the transcriptional level, which regulate metabolite accumulation to adapt to the new conditions (Hu et al., 2022). In a recent GWAS on mercury tolerance in

M. truncatula (Paape et al., 2022), we identified a UGT gene as a candidate gene within the proximity to the top SNP related to Hg tolerance. There were other UGT genes in the same region of chromosome 2, whose substrates are unknown. These results suggest that flavonoids and their glycoconjugates can have an important role in the response to Hg. In the present work, metabolomic data can help to uncover the molecular mechanisms at the metabolite expression level, underlying flavonoid accumulation in *M. truncatula* in response to Hg stress.

Thus, metabolomic data analyses suggest that significant variations in the flavonoids profile of the studied varieties are altered upon Hg treatment, affecting differently to leaf and root tissues as described above. In tomato plants subjected to heavy metal stress (zinc and copper), an increase in flavonoid accumulation could be observed; however, in this case the highest accumulation occurred in leaves compared to roots (Badiaa et al., 2020). An increase of flavonoid content in cotyledons occurs in buckwheat seedlings subjected to heavy metal stress. Interestingly, heavy metal-tolerant buckwheat cultivars present higher flavonoid accumulation levels than sensitive cultivars (Horbowicz et al., 2013).

The flavonoid biosynthetic pathway has been clearly delineated in some model plants like *M. truncatula*. On the basis of this model, a pathway diagram was constructed showing the differentially expressed flavonoids in the studied varieties of *M. truncatula* leaf and root samples. A total of 11 classes of identified flavonoids were mapped, along with their related genes and metabolic precursors, in the biosynthetic pathway (Figure 9). Differentially expressed aglycones and glycosylated derivatives are displayed in boxes, one for each target sample (L1, L2, L3, L4, R1, R2, R3, R4), using a color code from green (downregulated) to red (upregulated) based on Log_2FC value. The very first step in the phenylpropanoid pathway is catalysed by the enzyme phenylalanine ammonia lyase (PAL), and PAL expression has been reported to be induced by heavy metals; however, it is possible that this induction leads to enhanced phenolic acids accumulation, without necessarily affecting flavonoid biosynthesis (Ma et al., 2016; Berni et al., 2019). In the diagram presented in Figure 9, we consider, naringenin chalcone the first compound in the flavonoid biosynthetic pathway. Naringenin chalcone is transformed into naringenin – a core metabolite of the flavonoid pathway- via the enzymatic activity of chalcone isomerase. The metabolomic data did not show deregulation at this point of the route, which suggests that the phenylpropanoid pathways is not affected. The resulting flavanone naringenin, serves as a substrate for isoflavone synthase (IFS), flavone synthase (FNS), and flavanone 3-hydroxylase (F3H) to produce isoflavones, flavones and (dihydro)flavonols, respectively, (Gholami et al., 2014). Under heavy metal stress, flavonoid accumulation in plants is typically induced via the transcriptional regulation of biosynthesis genes (Naing and Kim, 2021 and references therein).

The first step of isoflavonoid biosynthesis begins with an oxidative aryl migration from C-2 to C-3, catalyzed by IFS enzyme to form the 2-hydroxyisoflavanone intermediates, and subsequent dehydration by 2HID to generate isoflavones

like genistein and daidzein. This “undecorated” isoflavones are precursors of the 4'-O-methylated forms biochanin A and formononetin, respectively, which are major isoflavonoid aglycones detected in *M. truncatula* roots (Figure 3). Further modifications in the A-ring, generate aglycones such as afrormosin and irisolidone, the first one derived from formononetin. The metabolomic results reveal that isoflavone biosynthesis is the most affected metabolic route in flavonoids pathways upon mercury stress. The five detected isoflavone aglycones show upregulated levels in at least three of the studied varieties, mainly in root samples, suggesting increased levels in the activity of IFS and 2HID enzymes. Glycosylated forms of biochanin A and formononetin were also found to be significantly upregulated, evidencing the metabolic interconnection and relevance of these isoflavones in the secondary metabolism of *M. truncatula*.

Pterocarpan form a class of isoflavonoid derivatives in which the B-ring is coupled to the C-ring via a furan ring. The biosynthesis of medicarpin, the pterocarpan detected in the *M. truncatula* root samples, starts with the conversion of formononetin to 20-hydroxyformononetin, catalyzed by the P450 enzyme I2'H. The upregulated levels of the glycosylated derivatives of medicarpin is consistent with the altered levels of its isoflavone precursor formononetin and glucoside and malonylglucoside forms. Peonidin glucosides are the only anthocyanidin-type flavonoids identified in the studied *M. truncatula* samples, and accumulated mainly in leaves. The biosynthesis of anthocyanidins and their precursor flavonols is mainly controlled by B-ring hydroxylation enzymes such as F3H, followed by dihydroflavonol-4-reductase and anthocyanidin synthase that converts the leucoanthocyanidins to the corresponding anthocyanidins. This branch of the pathway shows deregulation in the glycosylation levels of peonidin, suggesting and impairment in the anthocyanidin glycosylation process of leave tissues.

The biosynthesis of flavones is the second most affected route in *M. truncatula*, as a result of the Hg treatment, occurring mostly in leaf tissues where they are mainly accumulated. Flavones biosynthesis from flavanones occurs by introducing a double bond between C-2 and C-3, that is catalyzed by FNS via 2-hydroxyflavanone intermediate. Three types of flavones, namely apigenin, triclin, and chrysoeriol have been detected in *M. truncatula* samples in their glycoconjugated forms. Despite being major flavonoids in leaves, apigenin, and triclin glycoside levels were shown to be unaltered in the aerial part, upon Hg stress. On the contrary, the levels of these conjugated flavonoids were mainly deregulated in root tissues.

Flavonoids can undergo different modifications, including acylations, hydroxylations, methoxylations, prenylations, or glycosylations (Dixon and Pasinetti, 2010). Glycosides are the most common form of flavonoid derivatives. From the metabolomic results, it is clear that almost all detected flavonoids in the analyzed *M. truncatula* samples are accumulated in their conjugated forms with one or more sugar moieties, and very often as acylated glycoconjugates. Glycosylation enhances the water solubility of flavonoids and is critical for the transport and sequestration of these compounds in the vacuole

a clear mobilization of flavonoid compounds (increase in flavonoid production) in response to stress generated by Hg, mainly in roots.

DATA AVAILABILITY STATEMENT

The original contributions presented in this study are included in the article/**Supplementary Material**, further inquiries can be directed to the corresponding authors.

AUTHOR CONTRIBUTIONS

JP and ML conceived of the study. AC, EI, ML, and JP supervised the experimental work. GA-R and AS carried out the experiments. GA-R wrote the first draft of the manuscript. AS and JP wrote sections of the manuscript. TP aided in interpreting the results and provided critical feedback. All authors contributed to manuscript revision, read, and approved the submitted version.

REFERENCES

- Ahmed, G. J., and Yang, Y. (2022). Anthocyanin-mediated arsenic tolerance in plants. *Environ. Pollut.* 292:118475. doi: 10.1016/j.envpol.2021.118475
- Akram, N. A., Shafiq, F., and Ashraf, M. (2017). Ascorbic acid—a potential oxidant scavenger and its role in plant development and abiotic stress tolerance. *Front. Plant Sci.* 8:613. doi: 10.3389/fpls.2017.00613/BIBTEX
- Alloway, B. J., and Alloway, B. J. (2013). “Sources of heavy metals and metalloids in soils,” in *Heavy Metals in Soils. Environmental Pollution*, Vol. 22, ed. B. Alloway (Dordrecht: Springer), 11–50. doi: 10.1007/978-94-007-4470-7_2
- Arregui, G., Hipólito, P., Pallol, B., Lara-Dampier, V., García-Rodríguez, D., Varela, H. P., et al. (2021). Mercury-tolerant ensifer medicae strains display high mercuric reductase activity and a protective effect on nitrogen fixation in medicago truncatula nodules under mercury stress. *Front. Plant Sci.* 11:2268. doi: 10.3389/fpls.2020.560768/BIBTEX
- Badiaa, O., Yssaad, H. A. R., and Topcuogul, B. (2020). Effect of heavy metals (copper and zinc on proline, polyphenols and flavonoids content of tomato (*Lycopersicon esculentum* Mill.). *Plant Arch.* 20, 2125–2137.
- Behr, M., Neutelings, G., el Jaziri, M., and Baucher, M. (2020). You want it sweeter: how glycosylation affects plant response to oxidative stress. *Front. Plant Sci.* 11:1443. doi: 10.3389/fpls.2020.571399/BIBTEX
- Berni, R., Luyckx, M., Xu, X., Legay, S., Sergeant, K., Hausman, J. F., et al. (2019). Reactive oxygen species and heavy metal stress in plants: impact on the cell wall and secondary metabolism. *Environ. Exp. Bot.* 161, 98–106. doi: 10.1016/j.envexpbot.2018.10.017
- Cesco, S., Neumann, G., Tomasi, N., Pinton, R., and Weisskopf, L. (2010). Release of plant-borne flavonoids into the rhizosphere and their role in plant nutrition. *Plant Soil* 329, 1–25. doi: 10.1007/s11104-009-0266-9
- Chae, E. L., Ahn, J. H., and Lim, J. (2006). Molecular genetic analysis of tandemly located glycosyltransferase genes, UGT73B1, UGT73B2, and UGT73B3, in *Arabidopsis thaliana*. *J. Plant Biol.* 49, 309–314. doi: 10.1007/BF03031161
- Coba de la Peña, T. C., and Pueyo, J. J. (2012). Legumes in the reclamation of marginal soils, from cultivar and inoculant selection to transgenic approaches. *Agron. Sustain. Dev.* 32, 65–91. doi: 10.1007/S13593-011-0024-2
- Dixon, R. A., and Pasinetti, G. M. (2010). Flavonoids and isoflavonoids: from plant biology to agriculture and neuroscience. *Plant Physiol.* 154, 453–457. doi: 10.1104/PP.110.161430
- Farag, M. A., Huhman, D. V., Lei, Z., and Sumner, L. W. (2007). Metabolic profiling and systematic identification of flavonoids and isoflavonoids in roots and cell suspension cultures of *Medicago truncatula* using HPLC-UV-ESI-MS and GC-MS. *Phytochemistry* 68, 342–354. doi: 10.1016/j.phytochem.2006.10.023

FUNDING

This research was supported by grants from Agencia Estatal de Investigación, Spain (AGL2017-88381-R and PID2021-125371OB-I00) to JP and ML. GA-R would like to acknowledge the Ministry of Economy and Competitiveness for a “Juan de la Cierva-Incorporación” postdoctoral grant.

ACKNOWLEDGMENTS

We acknowledge support of 25% of the publication fee by the CSIC Open Access Publication Support Initiative through its Unit of Information Resources for Research (URICI).

SUPPLEMENTARY MATERIAL

The Supplementary Material for this article can be found online at: <https://www.frontiersin.org/articles/10.3389/fpls.2022.933209/full#supplementary-material>

- García de la Torre, V. S., Coba de la Peña, T., Lucas, M. M., and Pueyo, J. J. (2013). Rapid screening of *Medicago truncatula* germplasm for mercury tolerance at the seedling stage. *Environ. Exp. Bot.* 91, 90–96. doi: 10.1016/j.envexpbot.2013.03.004
- Gholami, A., de Geyter, N., Pollier, J., Goormachtig, S., and Goossens, A. (2014). Natural product biosynthesis in *Medicago* species. *Nat. Product Rep.* 31, 356–380. doi: 10.1039/c3np70104b
- Gill, S. S., and Tuteja, N. (2010). Reactive oxygen species and antioxidant machinery in abiotic stress tolerance in crop plants. *Plant Physiol. Biochem.* 48, 909–930. doi: 10.1016/j.plaphy.2010.08.016
- Harborne, J. B., and Baxter, H. (1999). *The Handbook Of Natural Flavonoids*. Hoboken, NJ: Wiley.
- Horbowicz, M., Dębski, H., Wiczowski, W., Szawara-Nowak, D., Koczkodaj, D., Mitrus, J., et al. (2013). The impact of short-term exposure to Pb and Cd on flavonoid composition and seedling growth of common buckwheat cultivars. *Polish J. Environ. Stud.* 22, 1723–1730.
- Hu, H., Fei, X., He, B., Luo, Y., Qi, Y., and Wei, A. (2022). Integrated analysis of metabolome and transcriptome data for uncovering flavonoid components of zanthoxylum bungeanum maxim. leaves under drought stress. *Front. Nutr.* 8:801244. doi: 10.3389/fnut.2021.801244
- Jasiński, M., Kachlicki, P., Rodziejewicz, P., Figlerowicz, M., and Stobiecki, M. (2009). Changes in the profile of flavonoid accumulation in *Medicago truncatula* leaves during infection with fungal pathogen *Phoma medicaginis*. *Plant Physiol. Biochem.* 47, 847–853. doi: 10.1016/j.plaphy.2009.05.004
- Khan, A., Khan, S., Khan, M. A., Qamar, Z., and Waqas, M. (2015). The uptake and bioaccumulation of heavy metals by food plants, their effects on plants nutrients, and associated health risk: a review. *Environ. Sci. Pollut. Res. Int.* 22, 13772–13799. doi: 10.1007/S11356-015-4881-0
- Kowalska, I., Stochmal, A., Kapusta, I., Janda, B., Pizca, C., Piacente, S., et al. (2007). Flavonoids from barrel medic (*Medicago truncatula*) aerial parts. *J. Agric. Food Chem.* 55, 2645–2652. doi: 10.1021/jf063635b
- Lee, H. K., Mysore, K. S., and Wen, J. (2018). Tnt1 insertional mutagenesis in *Medicago truncatula*. *Methods Mol. Biol.* 1822, 107–114. doi: 10.1007/978-1-4939-8633-0_7
- Li, P., Li, Y. J., Zhang, F. J., Zhang, G. Z., Jiang, X. Y., Yu, H. M., et al. (2017). The *Arabidopsis* UDP-glycosyltransferases UGT79B2 and UGT79B3, contribute to cold, salt and drought stress tolerance via modulating anthocyanin accumulation. *Plant J.* 89, 85–103. doi: 10.1111/TPJ.13324
- Ma, C., Liu, H., Guo, H., Musante, C., Coskun, S. H., Nelson, B. C., et al. (2016). Defense mechanisms and nutrient displacement in *Arabidopsis thaliana* upon

- exposure to CeO₂ and In₂O₃ nanoparticles. *Environ. Sci. Nano* 3, 1369–1379. doi: 10.1039/C6EN00189K
- Marczak, L., Stobiecki, M., Jasiński, M., Oleszek, W., and Kachlicki, P. (2010). Fragmentation pathways of acylated flavonoid diglucuronides from leaves of *Medicago truncatula*. *Phytochem. Anal.* 21, 224–233. doi: 10.1002/pca.1189
- Mierziak, J., Kostyn, K., and Kulma, A. (2014). Flavonoids as important molecules of plant interactions with the environment. *Molecules* 19, 16240–16265. doi: 10.3390/MOLECULES191016240
- Modolo, L. V., Blount, J. W., Achnine, L., Naoumkina, M. A., Wang, X., and Dixon, R. A. (2007). A functional genomics approach to (iso)flavonoid glycosylation in the model legume *Medicago truncatula*. *Plant Mol. Biol.* 64, 499–518. doi: 10.1007/s11103-007-9167-6
- Muñoz, W., Chavez, W., Pabón, L. C., Rendón, M. R., Patricia-Chaparro, M., and Otálvaro-Álvarez, Á. M. (2015). Extracción de compuestos fenólicos con actividad antioxidante a partir de Champa (Campomanesia lineatifolia). *Rev. CENIC Cienc. Químicas* 46, 38–46.
- Naing, A. H., and Kim, C. K. (2021). Abiotic stress-induced anthocyanins in plants: their role in tolerance to abiotic stresses. *Physiol. Plant.* 172, 1711–1723. doi: 10.1111/ppl.13373
- Nonnoi, F., Chinnaswamy, A., García de la Torre, V. S., Coba de la Peña, T., Lucas, M. M., and Pueyo, J. J. (2012). Metal tolerance of rhizobial strains isolated from nodules of herbaceous legumes (*Medicago* spp. and *Trifolium* spp.) growing in mercury-contaminated soils. *Appl. Soil Ecol.* 61, 49–59. doi: 10.1016/j.apsoil.2012.06.004
- Oldroyd, G. E. D., Harrison, M. J., and Udvardi, M. (2005). Peace talks and trade deals. Keys to long-term harmony in legume-microbe symbioses. *Plant Physiol.* 137, 1205–1210. doi: 10.1104/PP.104.057661
- Ortega-Villasante, C., Hernández, L. E., Rellán-Álvarez, R., del Campo, F. F., and Carpena-Ruiz, R. O. (2007). Rapid alteration of cellular redox homeostasis upon exposure to cadmium and mercury in alfalfa seedlings. *New Phytol.* 176, 96–107. doi: 10.1111/J.1469-8137.2007.02162.X
- Ortega-Villasante, C., Rellán-Álvarez, R., del Campo, F. F., Carpena-Ruiz, R. O., and Hernández, L. E. (2005). Cellular damage induced by cadmium and mercury in *Medicago sativa*. *J. Exp. Bot.* 56, 2239–2251. doi: 10.1093/JXB/ERI223
- Paape, T., Heiniger, B., Santo Domingo, M., Clear, M. R., Lucas, M. M., and Pueyo, J. J. (2022). Genome-wide association study reveals complex genetic architecture of cadmium and mercury accumulation and tolerance traits in *Medicago truncatula*. *Front. Plant Sci.* 12:806949. doi: 10.3389/fpls.2021.806949
- Panche, A. N., Diwan, A. D., and Chandra, S. R. (2016). Flavonoids: an overview. *J. Nutr. Sci.* 5, 1–15. doi: 10.1017/JNS.2016.41
- Patra, M., and Sharma, A. (2000). Mercury toxicity in plants. *Bot. Rev.* 66, 379–422. doi: 10.1007/BF02868923
- Peng, H., Chen, Y., Weng, L., Ma, J., Ma, Y., Li, Y., et al. (2019). Comparisons of heavy metal input inventory in agricultural soils in North and South China: a review. *Sci. Total Environ.* 660, 776–786. doi: 10.1016/J.SCITOTENV.2019.01.066
- Peralta-Videa, J. R., Lopez, M. L., Narayan, M., Saupe, G., and Gardea-Torresdey, J. (2009). The biochemistry of environmental heavy metal uptake by plants: implications for the food chain. *Int. J. Biochem. Cell Biol.* 41, 1665–1677. doi: 10.1016/J.BIOCEL.2009.03.005
- Rauter, A. P., Lopes, R. G., and Martins, A. (2019). C-Glycosylflavonoids: identification, bioactivity and synthesis. *Nat. Prod. Commun.* 2, 1175–1196.
- Schliemann, W., Ammer, C., and Strack, D. (2008). Metabolite profiling of mycorrhizal roots of *Medicago truncatula*. *Phytochemistry* 69, 112–146. doi: 10.1016/j.phytochem.2007.06.032
- Stanton-Geddes, J., Paape, T., Epstein, B., Briskine, R., Yoder, J., Mudge, J., et al. (2013). Candidate genes and genetic architecture of symbiotic and agronomic traits revealed by whole-genome, sequence-based association genetics in *Medicago truncatula*. *PLoS One* 8:e65688. doi: 10.1371/JOURNAL.PONE.0065688
- Staszuk, A., Swarczewicz, B., Banasiak, J., Muth, D., Jasiński, M., and Stobiecki, M. (2011). LC/MS profiling of flavonoid glycoconjugates isolated from hairy roots, suspension root cell cultures and seedling roots of *Medicago truncatula*. *Metabolomics* 7, 604–613. doi: 10.1007/s11306-011-0287-2
- Taguchi, G., Fujikawa, S., Yazawa, T., Kodaira, R., Hayashida, N., Shimosaka, M., et al. (2000). Scopoletin uptake from culture medium and accumulation in the vacuoles after conversion to scopolin in 2,4-D-treated tobacco cells. *Plant Sci.* 151, 153–161. doi: 10.1016/S0168-9452(99)00212-5
- Tang, H., Krishnakumar, V., Bidwell, S., Rosen, B., Chan, A., Zhou, S., et al. (2014). An improved genome release (version Mt4.0) for the model legume *Medicago truncatula*. *BMC Genomics* 15:312. doi: 10.1186/1471-2164-15-312
- Young, N. D., Debellé, F., Oldroyd, G. E. D., Geurts, R., Cannon, S. B., Udvardi, M. K., et al. (2011). The *Medicago* genome provides insight into the evolution of rhizobial symbioses. *Nature* 480, 520–524. doi: 10.1038/nature10625
- Zhang, J., Subramanian, S., Stacey, G., and Yu, O. (2009). Flavones and flavonols play distinct critical roles during nodulation of *Medicago truncatula* by *Sinorhizobium meliloti*. *Plant J.* 57, 171–183. doi: 10.1111/J.1365-313X.2008.03676.X
- Zhang, X., and Liu, C.-J. (2014). Multifaceted regulations of gateway enzyme phenylalanine ammonia-lyase in the biosynthesis of phenylpropanoids. *Mol. Plant* 8, 17–27. doi: 10.1093/MP/SSU134
- Zhao, J. (2015). Flavonoid transport mechanisms: how to go, and with whom. *Trends Plant Sci.* 20, 576–585. doi: 10.1016/J.TPLANTS.2015.06.007
- Zhao, J., and Dixon, R. A. (2010). The 'ins' and 'outs' of flavonoid transport. *Trends Plant Sci.* 15, 72–80. doi: 10.1016/j.tplants.2009.11.006
- Zhao, M., Jin, J., Gao, T., Zhang, N., Jing, T., Wang, J., et al. (2019). Glucosyltransferase CsUGT78A14 regulates flavonols accumulation and reactive oxygen species scavenging in response to cold stress in *Camellia sinensis*. *Front. Plant Sci.* 10:1675. doi: 10.3389/FPLS.2019.01675
- Zheng, Y. Z., Deng, G., Liang, Q., Chen, D. F., Guo, R., and Lai, R. C. (2017). Antioxidant activity of quercetin and its glucosides from propolis: a theoretical study. *Sci. Rep.* 7, 1–11. doi: 10.1038/s41598-017-08024-8
- Zhou, Z. S., Huang, S. Q., Guo, K., Mehta, S. K., Zhang, P. C., and Yang, Z. M. (2007). Metabolic adaptations to mercury-induced oxidative stress in roots of *Medicago sativa* L. *J. Inorg. Biochem.* 101, 1–9. doi: 10.1016/J.JINORGBIO.2006.05.011
- Zhou, Z. S., Wang, S. J., and Yang, Z. M. (2008). Biological detection and analysis of mercury toxicity to alfalfa (*Medicago sativa*) plants. *Chemosphere* 70, 1500–1509. doi: 10.1016/J.CHEMOSPHERE.2007.08.028

Conflict of Interest: The authors declare that the research was conducted in the absence of any commercial or financial relationships that could be construed as a potential conflict of interest.

Publisher's Note: All claims expressed in this article are solely those of the authors and do not necessarily represent those of their affiliated organizations, or those of the publisher, the editors and the reviewers. Any product that may be evaluated in this article, or claim that may be made by its manufacturer, is not guaranteed or endorsed by the publisher.

Copyright © 2022 Alvarez-Rivera, Sanz, Cifuentes, Ibáñez, Paape, Lucas and Pueyo. This is an open-access article distributed under the terms of the Creative Commons Attribution License (CC BY). The use, distribution or reproduction in other forums is permitted, provided the original author(s) and the copyright owner(s) are credited and that the original publication in this journal is cited, in accordance with accepted academic practice. No use, distribution or reproduction is permitted which does not comply with these terms.